Acta Materialia 126 (2017) 520–527

Contents lists available at ScienceDirect

Acta Materialia

journal homepage: www.elsevier.com/locate/actamat

Full length article

# Probing electrocolored Fe-doped $SrTiO_3$ bulks using optical second harmonic generation

D. Ascienzo [a, b], S. Greenbaum [a, b], T.J.M. Bayer [c], C.A. Randall [c], Y.H. Ren [a, b, *]

[a] Physics & Astronomy, Hunter College, The City University of New York, 695 Park Avenue, New York, NY 10065, USA
[b] The Graduate Center, The City University of New York, 365 5th Ave., New York, NY 10016, USA
[c] Materials Science and Engineering, Pennsylvania State University, University Park, PA 16802, USA

ARTICLE INFO

*Article history:*
Received 26 October 2016
Accepted 4 January 2017
Available online 5 January 2017

*Keywords:*
$SrTiO_3$
Electrocoloration
Oxygen vacancies
Perovskites
Second harmonic generation

ABSTRACT

We have investigated the spatial distribution of non-centrosymmetric defects in the electrocolored bulks of oxidized and reduced *Fe*-doped *$SrTiO_3$* (Fe:STO) single crystals by optical second harmonic generation (SHG) spectroscopy in the transmission geometry. Transmitted SHG intensities were examined across the anodic, mixed, and cathodic bulk regions of both Fe:STO crystals. The obtained nonlinear susceptibility ratios show that the structural distortions in the anodic and cathodic bulks of the electrocolored crystals are dominated by Fe:Ti—O bond bending around $Fe^{4+}$ defect centers and Fe:Ti—O bond stretching around $Fe^{3+}$ defect centers, respectively. Moreover, we identified a stronger local strain field at the color front of the oxidized crystal over the reduced one. This is attributed to more efficient strain relaxation during oxygen vacancy demixing in the reduced crystal.

## 1. Introduction

Perovskite-type dielectrics and ferroelectrics continue to be heavily studied for their applications in electroceramic devices such as capacitors, thermistors, actuators, and sensors [1]. In order to improve the durability and efficiency of these devices it is crucial to understand degradation and breakdown mechanisms induced by high *dc*-voltage and/or temperature stresses. Most recently, theoretical models based on defect chemistry and ionic transport have pointed to the electromigration of oxygen vacancies as a dominant contributor to aging, fatigue, and resistance degradation in these materials [2–6]. As a prototypical perovskite, *Fe*-doped *$SrTiO_3$* (Fe:STO) serves as an excellent material for studying the electrochemical and correlated structural effects related to oxygen vacancy electromigration. Under an imposed *dc*-voltage, Fe:STO undergoes a demixing process in which oxygen vacancies migrate towards the cathode while oxygen ions migrate towards the anode. This electromigration results in the formation of an Fe oxidation state gradient where the concentration of $Fe^{4+}$ is highest at the anode and lowest at the cathode, leading to a visible change in the optical absorption spectrum across the crystal, known as electrocoloration [5,7,8]. Another consequence of oxygen vacancy demixing is the formation of an electrochemically induced *p*-*n* junction where the anodic bulk is *p*-type conducting and the cathodic bulk is *n*-type conducting. The increase in conductivity of both regions ultimately leads to resistance degradation in the material [3–5].

Optical second harmonic generation (SHG) is a nonlinear spectroscopic technique which can be used as a probe for studying structural distortions in dielectric and ferroelectric crystals [9]. In the process of SHG, two photons of frequency $\omega$ are absorbed and a photon of frequency $2\omega$ is emitted. This process is forbidden in crystal point groups exhibiting a center of inversion symmetry, *i.e.* crystal symmetry indistinguishable under the operation $\mathbf{r} \rightarrow -\mathbf{r}$ [10–13]. This property makes optical SHG an effective tool for investigating the formation of non-centrosymmetric defects and strain at the unit cell scale in degraded perovskite-type oxides [14–16].

As a local symmetry probe, optical SHG in the reflection geometry was recently used to investigate structural inhomogeneity at the anode and cathode interfaces of electrically degraded oxidized and reduced Fe:STO single crystals [17]. The field-driven migration and aggregation of oxygen ions and vacancies were revealed to strongly affect the nonlinear optical responses from the interfaces. Both centrosymmetric $Fe^{4+}$:$Ti^{4+}$-$O_6$ octahedra and Jahn-Teller distortions were identified at the anode interfaces, while

---

* Corresponding author. Physics & Astronomy, Hunter College, the City University of New York, 695 Park Avenue, New York, NY 10065, USA.
*E-mail address:* yre@hunter.cuny.edu (Y.H. Ren).

http://dx.doi.org/10.1016/j.actamat.2017.01.007
1359-6454/

oxygen vacancy clusters led to a strong deviation from *4mm* group symmetry at the cathode interfaces. These nonlinear optical measurements provided important information on the structural inhomogeneity and defect concentration gradients formed at the degraded Fe:STO anode and cathode interfaces. However, structural changes inside the crystal bulks need to be addressed in order to better understand the degradation process.

In this paper, we report on our investigation of local structural broken symmetries within the anodic, mixed, and cathodic bulk regions of electrocolored Fe:STO single crystals by optical SHG in the transmission geometry. We measured the spatial distribution of the SHG intensities (*p*-in, *p*-out), (*s*-in, *p*-out), and (*d*-in, *s*-out) in the crystal bulks between the anode and cathode electrodes. We calculated the nonlinear susceptibility ratios, $|\chi_{zxx}/\chi_{zzz}|$, $|\chi_{xxz}/\chi_{zxx}|$, and $|\chi_{xxz}/\chi_{zzz}|$ and show that the structural distortions in the anodic and cathodic bulks of the electrocolored crystals are dominated by Fe:Ti—O bond bending around $Fe^{4+}$ defect centers and the Fe:Ti—O bond stretching around $Fe^{3+}$ defect centers, respectively. Higher SHG intensities were collected from the mixed bulk regions compared to the anodic and cathodic bulk regions. This is attributed to the formation of strain fields at the color fronts due to closely packed $Fe^{4+}$:$Ti^{4+}$-$O_6$ and $Fe^{3+}$:$Ti^{4+}$-$O_6$ octahedra. A stronger local strain field is revealed at the color front of the oxidized crystal over the reduced one. This is attributed to strain relaxation from a more efficient oxygen vacancy demixing process in the reduced crystal.

## 2. Experiment and theory

Verneuil-grown single crystals of (100) *$SrTiO_3$* doped with 0.01 wt% *Fe* were cut into 5 × 5 × 0.5 $mm^3$ pieces and epi-polished (MTI corporation, Richmond, CA). The Fe:STO single crystals were annealed in a tube furnace at a temperature of 900 °C under $pO_2 = 0.2$ bar and $pO_2 = 2 \times 10^{-5}$ bar for oxidation and reduction, respectively. Afterwards, the oxidized (B056) crystal was quenched in air ($pO_2 = 0.2$ bar) while the reduced (B057) crystal was quenched in argon ($pO_2 = 2 \times 10^{-5}$ bar) at 25 °C to freeze-in defect concentrations. As a result of the annealing and quenching procedures, B056 had a larger $[Fe^{4+}]$ than B057, which in turn had a larger $[Fe^{3+}]$ and $[V_O^{\cdot\cdot}]$ prior to degradation (Table 1). For the electrical degradation process, 100 nm thick platinum electrodes were deposited onto opposite, 0.5 × 5 $mm^2$, lateral faces of each crystal for *dc*-field application. Both samples were placed in a temperature bath of 210 °C under an applied *dc*-voltage of 100 V to induce the electromigration of oxygen ions and vacancies towards the anode and cathode interfaces, respectively [18]. Resistance degradation characteristics for B056 and B057 were recorded and are shown in Fig. 1. An increase in current density by two orders of magnitude, limited by the hole conductivity of the anode, was observed in both crystals [19,20].

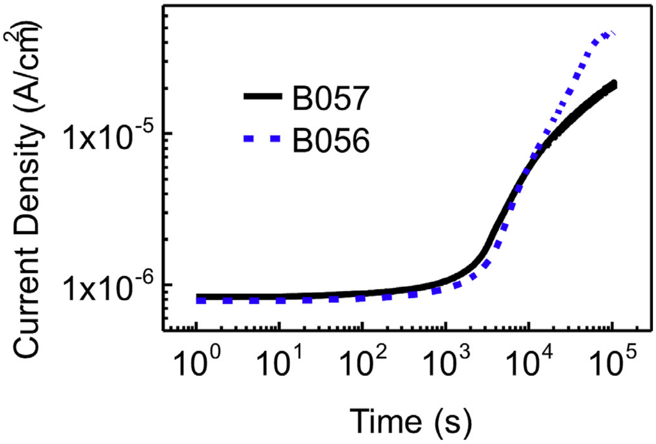

**Fig. 1.** Current density as a function of time across the oxidized (B056, quenched in air) and reduced (B057, quenched in argon) Fe:STO single crystals. Electrodegradation was performed at 210 °C under an imposed *dc*-voltage of 100 V.

Optical SHG measurements were performed in the transmission geometry at room temperature, after electrocoloration of the Fe:STO crystals. A mode-locked Ti:Sapphire ultrashort pulse laser (80 MHz, 10 nJ/pulse, 100 fs) was used as the fundamental light source (810 nm, ~10 μJ/$cm^2$) with a beam spot diameter of ~10 μm. Fig. 2 shows the experimental set-up for the detection geometry where the Fe:STO crystals were aligned with their surface normal axes at $\theta = 45^{\circ}$ with respect to the incident pump pulses traveling along the *xz*-plane. A Glan Polarizer acting as the analyzer and a band pass filter (Thorlabs, FB400-40) were placed in front of a photomultiplier tube module (Hamamatsu, H9305-04) for SHG light polarization selection and filtering out light at the fundamental frequency. A half-wavelength plate was used to rotate the polarization of the incident laser pulses, and the *p*-polarized (parallel to *xz*-plane) and *s*-polarized (perpendicular to *xz*-plane) SHG intensities were collected as functions of the incident light polarization angle. The *p*- and *s*-polarization axes for incoming fundamental and outgoing SHG light are marked in Fig. 3a. Images of the electrocolored crystals are shown in Fig. 3b. The dashed pink lines show the paths from which transmitted SHG intensities were measured on the respective samples. SHG intensities were measured at room temperature in the absence of an imposed *dc*-voltage so that all observed effects are due to the oxygen vacancy redistribution induced by the degradation process.

At room temperature, intrinsic *$SrTiO_3$* crystal bulk exhibits cubic (*Pm3m*) symmetry, although the structural symmetry of surface layers may transition to tetragonal (*4mm*) symmetry due to changes in atomic packing [11,21]. In electrically degraded Fe:$SrTiO_3$, the field-driven migration of oxygen vacancies and electrochemical changes of Fe defect centers lead to electrocoloration, as shown in Fig. 3b. The anodic bulk turns dark brown where oxidation occurs to form $Fe^{4+}$ centers and the cathodic bulk turns light brown where reduction occurs to form $Fe^{3+}$ centers [7,8,18]. These electrochemical changes combined with electrical and thermal stresses applied during degradation lead to tetragonal (*4mm*) defects in the crystal bulk. For the transmission geometry, the SHG coherence length, $L_{coh} = \frac{\lambda_\omega}{4(n^{2\omega} - n^{\omega})}$, is calculated to be ~660 nm for fundamental light of wavelength 810 nm; this is ~16.5 times longer than the coherence length in the reflection geometry [12]. Since the coherence length represents the effective depth that SHG radiation is generated from within the crystal, the transmitted SHG response is largely due to electric-dipole contributions from the non-centrosymmetric bulk while surface dipolar

**Table 1**
Tabulated concentration values in the oxidized (B056) and reduced (B057) crystals before degradation.

| Treatment | Sample/Region | $[V_O^{\cdot\cdot}](cm^{-3})$ | $[Fe^{3+}](cm^{-3})$ | $[Fe^{4+}](cm^{-3})$ |
|---|---|---|---|---|
| After Quenching | B056 | 1.03e18 | 2.06e18 | 2.52e18 |
| | B057 | 2.43e18 | 4.85e18 | 7.30e17 |